Hydro-plastic slamming

Zhaolong Yu & Jørgen Amdahl
Centre for Autonomous Marine Operations and Systems (AMOS), Norwegian University of Science and Technology (NTNU), Norway
Department of Marine Technology, Norwegian University of Science and Technology (NTNU), Norway.

ABSTRACT: Ships and offshore structures will unavoidably experience water impacts (slamming) throughout their service time. During slamming, the coupling between hydrodynamic pressure and the elastic structural response, termed as hydro-elasticity, has been studied extensively. However, when the structure is encountered by steep and energetic waves in extreme sea states, structural stresses may exceed the material yield stress, causing large plastic flow and structural damage. This hydro-elastoplastic slamming phenomenon has rarely been studied.

Recently, we formulated an analytical solution to the hydro-plastic response of beams and stiffened panels subjected to extreme water slamming (Yu et al., 2018a, Yu et al., 2018b), coupling the hydrodynamic loading and the structural response. The model assumes that in the extreme slamming events, plastic structural deformation energy is dominant and the elastic effect can be neglected. This paper briefly introduces the idea behind the analytical hydro-plastic slamming model. Non-dimensional parameters governing the hydro-plastic phenomenon are identified and discussed. A validation of the model is presented by comparison with multi-material Arbitrary Lagrangian Eulerian (ALE) simulations in LS-DYNA. The results are discussed. The resulting non-dimensional curves are good candidates as design curves for designing against extreme water slamming in Accidental Limit States (ALS).

Keyword: hydro-plastic slamming; analytical solution; beams and stiffened panels; permanent deflection; validation

1 INTRODUCTION

Water impacts are known to occur for ships and offshore structures at sea due to the relative motion between the liquid and the structure. Example scenarios leading to slamming are water entry and exit of ship bow and stern, offshore platforms subjected to steep breaking waves, high speed vessels travelling in waves and free-falling life boats. Structures subjected to impulsive loads from water slamming, may respond in the elastic or elastoplastic regimes depending on the load intensity. There can be significant coupling effect between water pressure and the structural response, termed as hydroelasticity and hydro-elastoplasticity, respectively. Hydroelastic slamming has been studied extensively, for instance by Faltinsen (2000), Kvalsvold and Faltinsen (1995), Bishop and Price (1979) and Qin and Batra (2009), but similar attention has not been given to the hydro-elastoplastic or hydro-plastic slamming. In practice, offshore structures may be impacted by steep and energetic waves in extreme sea states, causing significant structural damage. For example, the accident of the offshore drilling rig *COSL Innovator* in the North Sea in 2015 led to one death and extensive damage to the cabins after being struck by an energetic horizontal wave. In order to maintain structural safety and to prevent such accidents, rules and standards should be established for designing against extreme slamming loads.

For structural design subjected to slamming, simple guidelines were introduced in DNVGL-OTG-13 (2016) for the air gap calculation and in DNVGL-OTG-14 (2016) for providing the temporal and spatial distributions of the design slamming loads. The rules focus on the peak pressure, the shape of the pressure impulse, the impulse duration and the pressure spatial distribution. Similarly, a few researchers studied plastic response of structures subjected to extreme slamming by assuming a certain temporal and spatial pressure distribution, such as Jones

(2011), Jiang and Olson (1995) and Henke (1994). These methods, however, neglect the hydro-elastoplastic coupling between the structural response and water pressure, and do not reflect the real physics behind the phenomenon.

Limited knowledge exists for scenarios where the plastic response of a structure becomes dominant in the Accidental Limit States (ALS) conditions. In order to bridge the knowledge gap and to obtain a deeper understanding of the hydro-plastic slamming phenomenon, the authors (Yu et al., 2018a, Yu et al., 2018b) formulated an analytical solution for the hydro-plastic response of beams and stiffened panels subjected to extreme water slamming. This paper briefly introduces the idea behind the hydro-plastic slamming model, and verifies the proposed analytical model by means of multi-material ALE simulations using LS-DYNA. Water entry simulations are then carried out for the flat plate strips and stiffened panels with different cross sectional dimensions and impact velocities. The analytical model is discussed with respect to the fluid flow, the structural deflection, the pressure history, and the impulse. Potential application and limitations of the analytical method are discussed.

2 ANALYTICAL MODEL FOR HYDRO-PLASTIC SLAMMING

2.1 *The analytical model for hydro-plastic slamming*

We assume that in the extreme slamming events in ALS conditions, the elastic energy of a structure is small compared to the plastic energy such that all the kinetic energy should be dissipated by plastic deformations. The perfectly plastic material is often adopted in other ALS conditions with good accuracy, such as collisions and groundings (Yu and Amdahl, 2018). During hydro-plastic slamming of flat beams, the response is categorized into two phases, i.e. the structural inertia phase (also called the acoustic phase) and the free deflection phase. In the structural inertia phase, the structure is subjected to an intensive pressure impulse with a large pressure peak and a short duration. At the end of the structural inertia phase, the structure is assumed to be imparted a deformation velocity equal to the initial drop velocity V_0 in the beam middle portion between the two travelling hinges. The deformation velocity decreases linearly to zero from the travelling hinges to the beam ends. The duration of the structural-inertia phase is, however, too short for the structure to build up any deflection. These are considered as initial conditions of the free deflection phase.

In the free deflection phase, the structure deforms and may undergo three deformation stages, i.e. the travelling hinge stage 1, the stationary hinge stage 2 and the pure tension stage 3 (refer Fig. 1). In stage 1, travelling hinges form at a certain distance X from the beam ends and move towards the middle. The beam portion between the hinges has a constant velocity V_m equal to the initial impact velocity V_0 (refer Fig. 1(a)). When the travelling hinges merge in the middle, the stationary hinge stage 2 starts and the beam middle velocity starts to decrease over time. During the deflection, the beam bending moment and axial membrane force interact through the generalized interaction curves. For stiffened panels, the interaction functions are taken from Yu et al. (2018c). For beams fixed at the ends, when the beam middle deflection δ reaches the beam height h, the beam cross section becomes fully occupied by membrane forces, and the pure tensile stage 3 starts. Permanent deflection is reached when the beam middle velocity V_m decreases to zero.

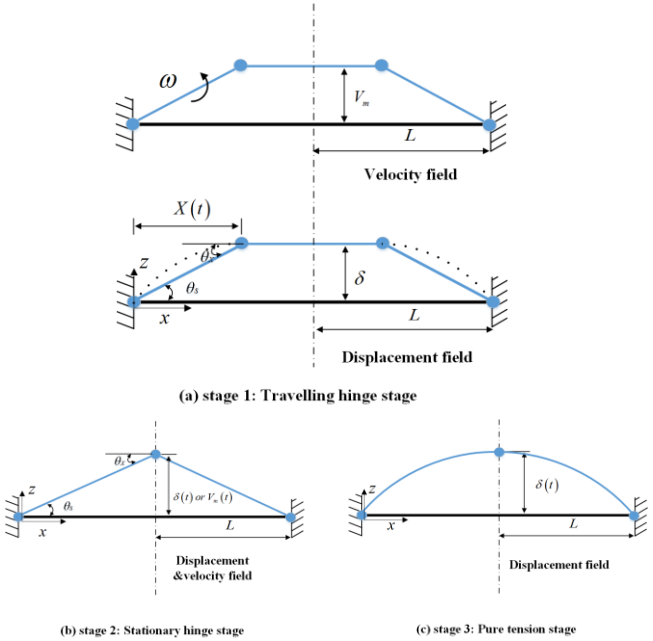

Fig. 1. Deformation stages of a beam during the free-deflection phase induced by slamming

During the deformations, significant coupling exists between the beam plastic deflection and the water pressure, denoted as hydro-plasticity. In stages 2 and 3, water pressure acts as an added mass effect and pushes the decelerating structure to deform. For stage 1, apart from an added-mass term, we have a second pressure term related to an added-mass time change effect due to the moving hinges leading to a change in the structural mode.

By equating the rate of internal and external works, the governing motion equations are found, and are solved numerically with the fourth order Rouge-Kutta method. The detailed formulation of the hydro-plastic slamming theory can be found in Yu et al. (2018a).

2.2 *Governing non-dimensional parameters*

For the hydro-plastic slamming response of flat plate strips, i.e. of two-dimensional (2D) flat plates, three governing non-dimensional parameters have been identified, which are,

- The non-dimensional velocity
$$V_{nd} = V_0\sqrt{\frac{\rho L^3}{M_0 h/b}}$$
- The mass ratio $m_{nd} = m/\rho bL$
- The ratio of initial travelling hinge position over half of the beam length
$$X_{nd} = \frac{X(t=0)}{L} = \sqrt{\frac{24}{\left(V_0\sqrt{\frac{\rho L^3}{M_0 h/b}}\right)^2}\cdot\frac{V_0 L}{c_e h}}$$

For the hydro-plastic response of stiffened panels, two more parameters are identified in addition to the three above:

- The area ratios:
$$A_{ps,nd} = A_p/A_s \text{ and } A_{wt,nd} = A_w/A_t$$

Here, V_0 is the initial impact velocity, ρ is the water density and L, b, h are, respectively, the length, width and height of the beam. m is the mass of a beam per unit length, $X(t=0)$ is the initial position of a travelling hinge from the corresponding beam edge. c_e is the speed of sound in water. M_0 is the fully plastic bending moment for the beam cross section. $M_0 = 1/4\sigma_y bh^2$ for rectangular beams and $M_0 = \sigma_y(A_t + A_w/2)h$ for stiffened panel cross sections. A_p, A_w, A_t are the area of the plate flange, area of the web and area of the top flange, respectively. $A_s = A_t + A_w$ is the area of the stiffener.

It is found that the non-dimensional velocity V_{nd} is the most crucial parameter that dominates the hydro-plastic response of beams and stiffened panels. Stiffened panels with large web heights, *h*, are mainly governed by stages 1 and 2 deformations. The permanent deflection δ_p/h increases nonlinearly with the non-dimensional velocity. For plates, the characteristic dimension *h* is much smaller than the stiffener spacing, and the response is mainly governed by stage 3. δ_p/h increases virtually linearly with the non-dimensional velocity.

The area ratios A_p/A_s and A_w/A_t are important parameters for stiffened panels. Permanent deflections increase with decreasing A_p/A_s and A_w/A_t ratios for a given non-dimensional velocity, and the A_p/A_s ratio is dominant. The influences of the mass ratio $m/\rho bL$ and the $X(t=0)/L$ ratio are generally limited.

3 NUMERICAL SET-UP OF ALE SIMULATIONS

3.1 *Numerical set-up of ALE simulations*

Water and air are modelled with multi-material Eulerian meshes while the structure is modelled with Lagrangian meshes. Coupling is enabled in a way that the Lagrangian structure domain imposes displacement and velocity boundary conditions on the Eulerian fluid, which in return imposes hydrodynamic pressure on the structure. The water and air domains are modelled using the 1 point ALE multi-material solid elements. Material properties of the fluids are defined with the NULL materials and EOS (equation of state). The properties adopted for water and air are listed in Table 1. The values have been validated by Bae and Zakki (2011) through comparison with experiments.

Table 1 EOS linear polynomial parameters for water and air, from Bae and Zakki (2011)

	Water	Air
Density (kg/m^3)	1025	1.225
C_0	0	0
C_1	$2.002\cdot10^9$	0
C_2	$8.436\cdot10^9$	0
C_3	$8.010\cdot10^9$	0
C_4	0.4394	0.4
C_5	1.3927	0.4
C_6	0	0
E_0	$2.086\cdot10^5$	$2.5\cdot10^5$
V_0	1	1

The penalty-based coupling method is applied to model contact between the fluid and the structure. During contact, the fluid nodes are allowed to have a small penetration into the structure. Resisting forces are then imposed between the contact points on the structural elements and the fluid nodes. The penalty factor corresponding to the contact stiffness of interacting bodies is set to the default value of 0.1. The contact damping is selected to be 0.9 times the critical damping according to Stenius et al. (2006). The fluid-structure coupling takes place in the normal direction to the body surface when the fluid tends to enter the structure, i.e. in compression only.

The numerical settings have been validated of reasonable accuracy in Yu et al. (2018b) by comparison with a 2D *rigid*-wedge drop test by Zhao et al.

(1996) and the drop test of a horizontal flat *elastic* plate by Faltinsen et al. (1997). A mesh size sensitivity analysis was carried out as well, and a mesh size of 10 mm and 20 mm are determined for the slamming simulation of plates and stiffened panels, respectively.

The steel material with a yield stress of 355 MPa is used for the plates and stiffened panels. A linear hardening model with a small hardening stiffness is used to reduce the influence of hardening as the analytical model assumes an elastic-perfectly plastic material. The parameters for the material are shown in Table 2.

Table 2. Material properties for the plates and stiffened panels

Material	*Hardening type*	σ_y *(MPa)*	*E (GPa)*	E_t *(MPa)*
steel	Linear	355	207	400

3.2 *Water entry of flat plates*

For the 2D water entry simulation of flat plates, a water domain with dimensions of 3 m×2 m and an air domain of 3 m×1 m were established (refer Fig. 2). The flat plate is 1m in length. The plate boundary nodes are fixed against all degrees of freedom except for the vertical *z* direction. One shell element is modelled in the thickness direction. The fluid nodes are fixed in *y* direction to enable a 2D condition The plate thickness is set as 3 mm, 6 mm, 10 mm or 20 mm with an initial impact velocity of 5 m/s, 10 m/s or 15 m/s.

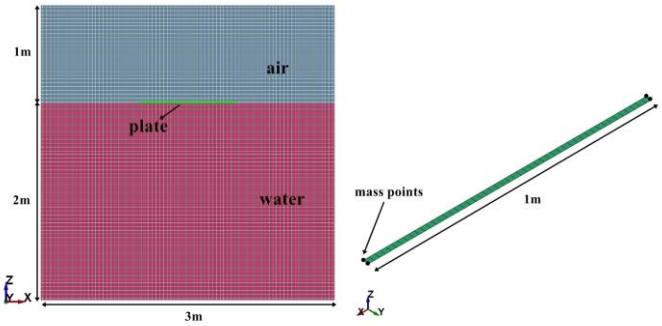

Fig. 2. Left: modelling of water entry of a flat plate; Right: numerical plate

3.3 *Water entry of stiffened panels*

For 2D water entry simulation of stiffened panels, the water and air domains are modeled with the dimensions of 4 m×2 m and 4 m×1.5 m, respectively, (refer Fig. 3). In the thickness direction, the domain extension equals the span between stiffeners. In order to verify the analytical model comprehensively, 6 stiffener cross sections are modelled, covering different area ratios, panel lengths and panel thicknesses.

The dimensions are given in Table 3. The panel stiffness varies from weak to strong, yielding large to small permanent deflections for a given initial impact velocity. Different cases for water entry of flat stiffened panels are simulated with the initial impact velocity being 7 m/s, 10 m/s or 15 m/s.

The fluid nodes are fixed in *y* direction to enable a 2D flow condition. The plate boundary nodes are fixed against all degrees of freedom except for the vertical *z* direction.

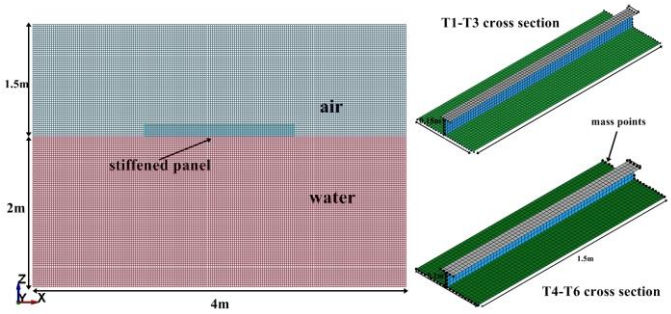

Fig. 3. Left: modelling of water entry of a stiffened panel. Right: different geometries of the numerical panel

Table 3. Stiffened panel dimensions (Unit: mm)

Cross section type	*Length*	*Plate flange*	*Web*	*Top flange*	A_p/A_s	A_w/A_t
T1	2000	600 x 5	150 x 10	100 x 10	1.2	1.5
T2	2000	600 x 10	150 x 10	100 x 10	2.4	1.5
T3	2000	600 x 15	150 x 15	100 x 15	2.4	1.5
T4	1500	500 x 8	100 x 8	100 x 8	2.5	1
T5	1500	500 x 10	100 x 15	100 x 15	1.67	1
T6	1500	500 x 15	100 x 20	100 x 20	1.875	1

4 COMPARISON OF THE ANALYTICAL MODEL AND NUMERICAL SIMULATIONS

4.1 *Water entry of flat plates*

The numerical predictions of fluid flow and plate deformations are shown in Fig. 4. The plate strips are 1 m in length and 0.02 m in width. The plate thickness is 6 mm and the initial impact velocity is 10 m/s. The corresponding displacement profiles for half a plate with a time interval of 0.4 ms are shown in Fig. 5. They demonstrate that the plate gets a significant change of curvature over a relatively short distance and may be interpreted as a plastic hinge. The instantaneous hinge position, which moves towards plate center with increasing time, is indicated with red points in Fig. 5. It is interesting to notice that the positions of the travelling hinge at different time instants lie virtually on a straight, horizontal line for a time period. This implies that, the deformation velocity at this stage averagely counteracts the drop velocity. This is a clear evidence that the initial deformation velocity is averagely equal to the drop velocity. In addition, the wider view confirms negligible plate deformations within less than 1ms from the initial impact.

To the left of the hinge, the imposed plastic curvature seems to be fairly constant, and the 'arm' behind the hinge rotates only as a rigid body. It is found that the rotating arms become no longer parallel to each other before the hinge reaches the beam middle. This is because, the deformation of the thin plate follows *Path 2*, where the pure tension stage 3 is reached but the moving hinges has not met in the middle. From Fig. 5, it seems that it takes more time to reach the pure tension stage in numerical simulations than predicted using the proposed theory. This is due to the large elastic deflections before entering the plastic regime, which is not accounted for in the theory. The plot confirms that the travelling hinge concept is useful in describing the actual displacement field.

With the imposed velocity from the acoustic phase, the plate builds up deformations over time in the free-deflection stage until all the energy is dissipated and the permanent deflection is reached. During this process, water is accelerated upwards, forming jets that leave from the structure sides. A small portion of elastic energy may be released through plate vibrations about the permanent deformations.

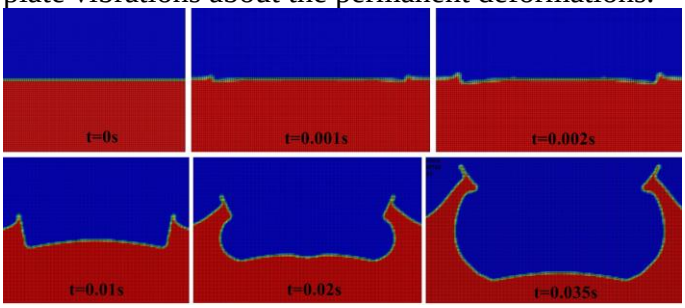

Fig. 4. Snapshots of plate deformation and flow field during water entry; the plate thickness is 6 mm and the initial impact velocity is 10 m/s

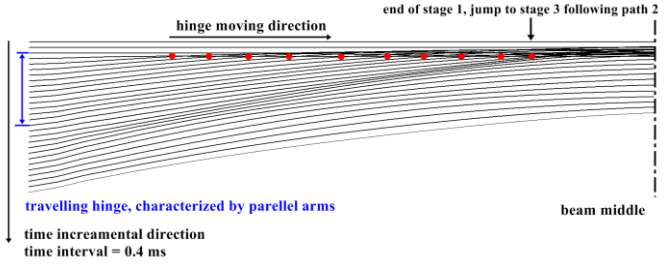

Fig. 5. Snapshots of displacement profiles for half of a plate strip during water entry; the plate thickness is 6 mm and the initial impact velocity is 10 m/s. The time interval is 0.4 ms. The red points denote the positions of the travelling hinge at each time instant.

Figs. 6 and 7 plot the average pressure histories for the flat plate with impact velocities of 5 m/s, 10 m/s and 15 m/s and with plate thicknesses of 3 mm, 6 mm, 10 mm and 20 mm. From Fig. 6, the peak pressure increases linearly with increasing impact velocity for given plate dimensions. The peak pressure, however, cannot exceed the acoustic pressure. Proportionality is also found for the impulse of the acoustic stage and the total impulse including the acoustic stage and the free deflection stage with respect to the impact velocities. This is consistent with the assumption, used in the analytical method, that in the acoustic stage, the structure is imparted an velocity equal to the initial impact velocity V_0 in the middle between travelling hinges and linearly decreasing to zero from the travelling hinge to the beam end. If we crudely assume the whole beam velocity is V_0, then the impulse in the acoustic stage would be $\rho_m h V_0$ $\left(\text{unit:Ns/m}^2\right)$. Here, ρ_m is the density of the structural material. Figs. 6 and 7 show that $\rho_m h V_0$ is 15%-25% smaller than the impulse in the acoustic stage $I_{acoustic}$.

Fig. 7 shows that the plate stiffness is a crucial factor to determine the peak pressure in the acoustic stage and the slamming duration. Given the same impact velocity of 10 m/s, the peak pressure and impulse of the acoustic stage increase with increasing plate thickness while the slamming duration reduces. It is interesting to find that the total impulse remains virtually the same regardless of the plate thickness.

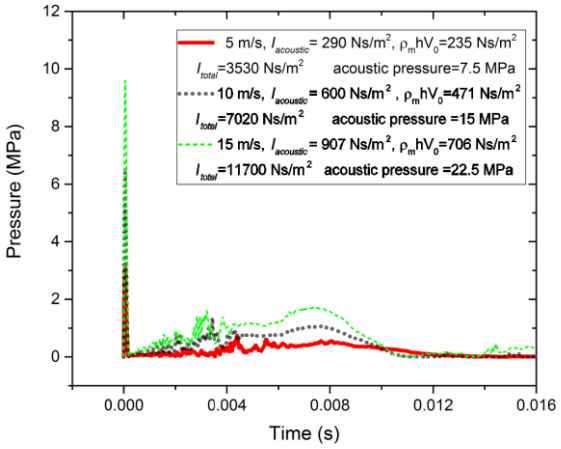

Fig. 6. Average pressure time history over plates with different initial impact velocities; each plate strip has the dimensions of 1 m×0.02 m×6 mm

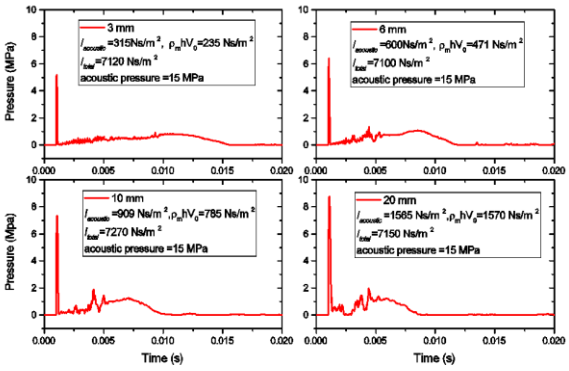

Fig. 7. Average pressure history versus plate thickness with an initial impact velocity of 10 m/s

Fig. 8 compares the central deflections of flat plates with a thickness of 3 mm, 6 mm, 10 mm and 20 mm during 2D water-entry as predicted by ALE simulations and by the proposed analytical model. The initial impact velocity is 10 m/s. The simula-

tions show that the plates deform to their permanent deflections with small elastic oscillations about the mean deformations, and the plastic energy is dominant. Fig. 9 shows the deflection history of the 6 mm plate with an initial impact velocity of 5 m/s, 10 m/s and 15 m/s. From Figs. 8 and 9, the permanent deflections predicted with the analytical model agree well with those from the ALE simulations for the selected plate thickness and impact velocity ranges. It is observed that the permanent deflection is somewhat overestimated especially for small impact velocities. This is mainly because the analytical model assumes that all energy is dissipated by the plastic deformation and the elastic energy is neglected. It is interesting to find from Figs. 6 and 9 that the durations of the acoustic and the free-deflection stage remain virtually insensitive to the initial impact velocity. Permanent deflections are reached virtually at the same time for all velocities.

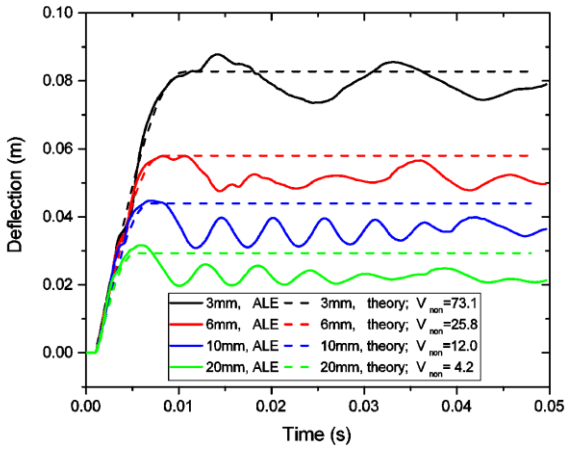

Fig. 8. Plate deflections for different thicknessnes during water entry with an initial velocity of 10 m/s

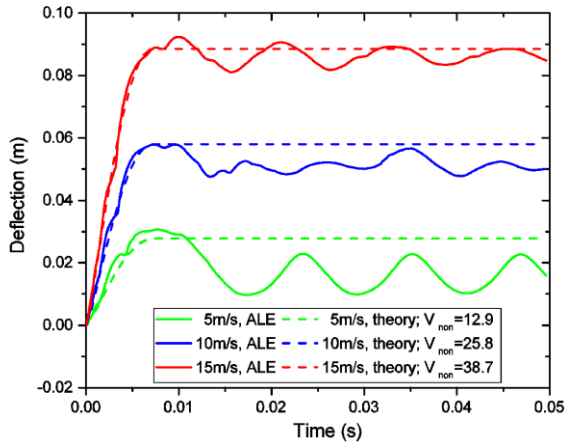

Fig. 9. Plate deflections for different initial velocities during water entry; plate thickness t = 6 mm

The non-dimensional permanent deflections of plate strips are plotted versus the non-dimensional velocity in Fig. 10 for different mass ratios. Reasonable agreement with ALE simulations is demonstrated. The numerical results confirm that the non-dimensional velocity is dominant. One of the ALE data point deviates slightly from the curve because the elastic energy becomes important in this case.

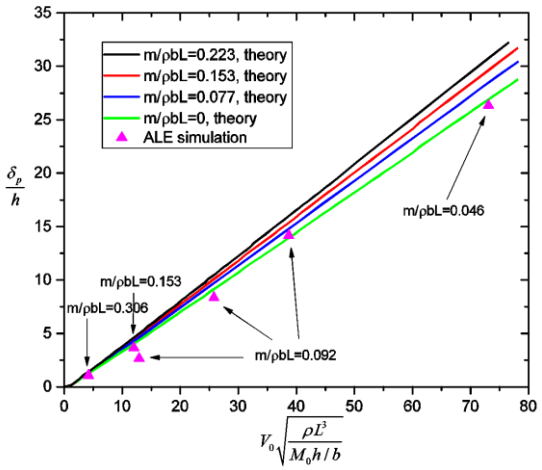

Fig. 10. Non-dimensional permanent deflection versus non-dimensional velocity curves from the analytical model and the corresponding data from ALE simulations during slamming

4.2 *Water entry of flat stiffened panels*

The general features of the fluid flow during water entry of stiffened panels are quite similar to those shown in Fig. 4 for flat plates. The T3 stiffened panel deformations with an initial impact velocity of 10 m/s are shown in Fig. 11. The panel is subjected to significant plastic flow at the supports and the beam middle span, and undergoes large plastic deformations.

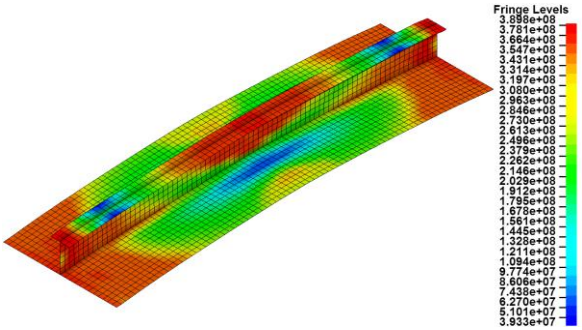

Fig. 11. Deformation of the T3 stiffened panel under slamming loads as predicted by the ALE simulation. The initial impact velocity is 10 m/s

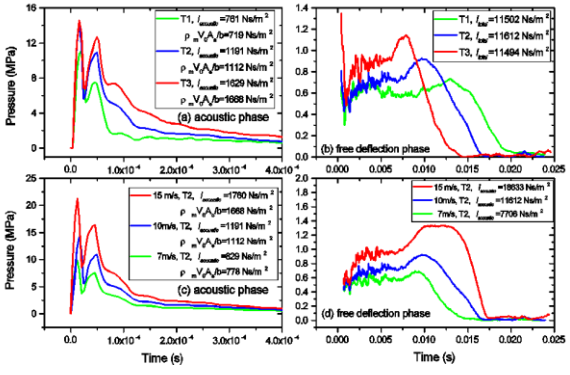

Fig. 12. Average pressure histories predicted by the ALE simulations for (a) stiffened panels T1-T3 with an initial drop veloc-

ity of 10 m/s in the acoustic phase, (b) stiffened panels T1-T3 with an initial drop velocity of 10 m/s in the free deflection phase, (c) stiffened panel T2 with different initial velocities in the acoustic phase, (d) stiffened panel T2 with different initial velocities in the free deflection phase

Time histories of the average pressure for panels with T1-T3 cross sections with an initial drop velocity of 10 m/s are plotted in Figs. 12 (a) and (b). The pressure histories for panel T2 are plotted as a function of the drop velocity in Figs. 12 (c) and (d). According to the velocity assumption, the momentum change due to the structural deformation is approximately $\rho_m V_0 A_e / b$ $\left(\text{unit:Ns/m}^2\right)$. The $\rho_m V_0 A_e / b$ values for stiffened panels are very close to the impulse predicted in the acoustic phase by the ALE simulations (refer Figs. 12 (a) and (c)). This justifies the assumption of an initial uniform deformation velocity equal to V_0 in the free deflection phase. Based on the similarity of the pressure impulse for rigid and deformable panels in the acoustic phase, it may become reasonable to measure the pressure impulse in the acoustic phase on rigid plates, and use the impulse to calculate the deformation velocity of the deformable structure. From Figs. 12 (c) and (d), the pressure histories are generally in phase while the magnitude increases with velocity. The impulses in the acoustic phase and the total impulses increase with the velocity as well.

Figs. 13 and 14 compare central deflections of flat stiffened panels with 6 different cross sections during 2D water entry predicted by LS-DYNA ALE simulations and by the analytical model. The stiffened panels cover different beam lengths, $A_p / \left(A_w + A_t\right)$ ratios and A_w / A_t ratios. The initial impact velocity is 10 m/s for T1-T3 stiffened panels and 15 m/s for T4-T6 stiffened panels. Figs. 15 and 16 compare the deflections for the T2 and T5 stiffened panels, respectively, with the initial impact velocity being 7 m/s, 10 m/s and 15 m/s.

The results show that the analytical model predicts the deflection curves of stiffened panels quite reasonably both in phase and in magnitude. It overestimates slightly the deflection for small impact speeds. One main reason is the rigid perfectly plastic material assumption adopted for the steel without considering the elastic effect. Another reason is that the initial position of the travelling hinge is determined by assuming that the peak pressure is equal to the acoustic pressure, but in reality the true pressure should be smaller (see e.g. Fig. 12). This underestimates the distance of the initial travelling hinge position to the supports, i.e. $X\left(t=0\right)$, and thus overestimates the permanent deflections. Considering the complexity of the problem, the proposed analytical model provides fairly good accuracy.

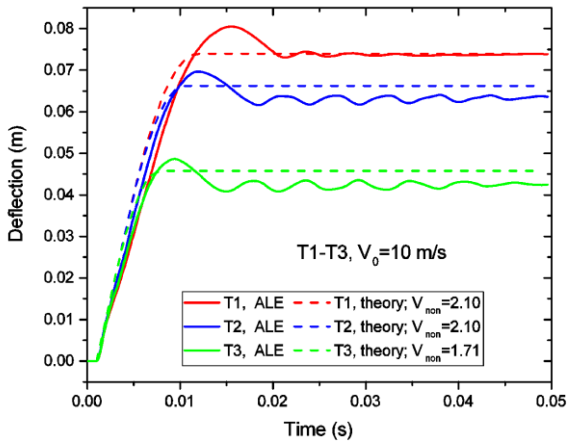

Fig. 13. Deflections of stiffened panels with cross sections of T1, T2 and T3 during water entry. The initial impact velocity is 10 m/s

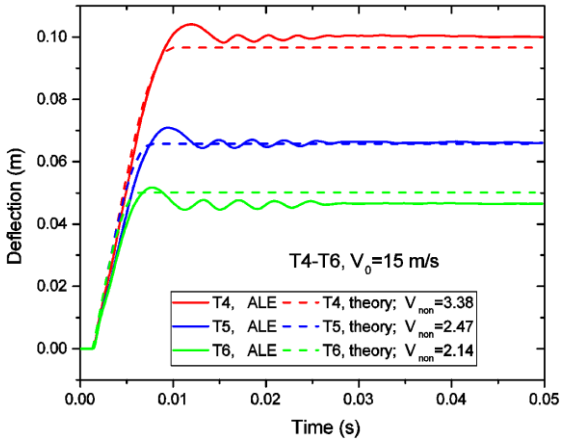

Fig. 14. Deflections of stiffened panels with cross sections of T4, T5 and T6 during water entry. The initial impact velocity is 15 m/s

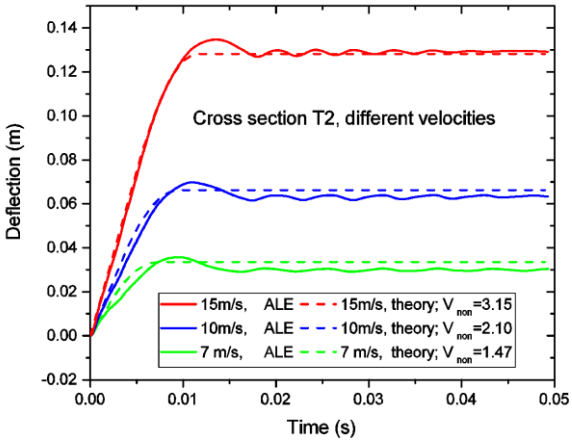

Fig. 15. Deflections of T2 stiffened panels with different initial impact velocities during water entry

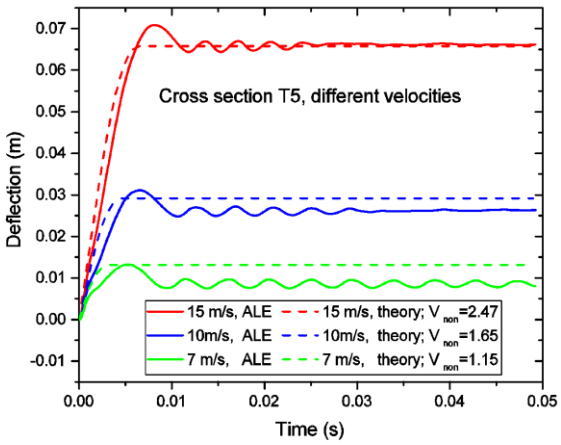

Fig. 16. Deflections of T5 stiffened panels with different initial impact velocities during water entry

Fig. 17 plots the non-dimensional permanent deflections versus the non-dimensional velocity for different A_p / A_s and A_w / A_t ratios for stiffened panels. The non-dimensional velocity is dominant, but the A_p / A_s and A_w / A_t ratios are also important. The design curves are compared with data points from ALE simulations. Results show that the non-dimensional curves compare reasonably with ALE simulations.

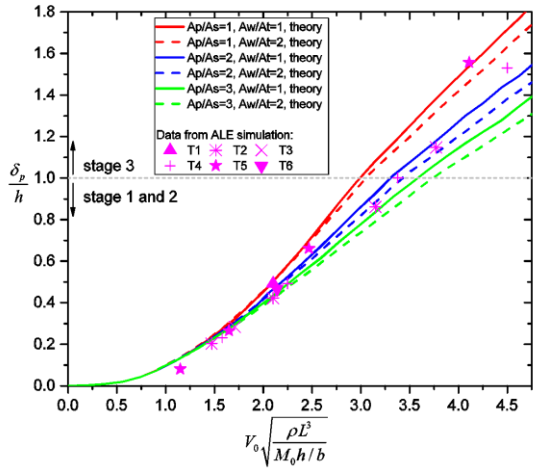

Fig. 17. Non-dimensional permanent deflection of stiffened panels versus non-dimensional velocity curves from the analytical model, and the data from ALE simulations during slamming

5 CONCLUSIONS

This paper presents the idea behind an analytical model for the hydro-plastic slamming of beams and stiffened panels and verifies the model by comparing model predictions with results from the multi-material ALE simulations. Hydro-elastoplastic simulations were carried out for beams and stiffened panels, and the results were discussed. The following conclusions are drawn:

1. The proposed hydro-plastic model is capable of predicting large inelastic permanent deflections of plates and stiffened panels during flat or nearly flat water impacts with good accuracy both in magnitude and in phase. The coupling between hydrodynamic loads and structural deformations is well captured.

2. A key element of the theoretical model is the travelling hinge concept used to describe the structural deformation. The validity of the concept is confirmed from the snapshots of displacement profiles of plate strips from the hydro-elastoplastic slamming ALE simulations.

3. In the acoustic stage, the maximum pressure increases with the impact velocity and the structural stiffness, and the impulse imparted to the structures is close to the structural momentum with a deformation velocity equal to the initial impact velocity. In the free deflection phase, the interaction with hydrodynamic actions is important. The pressure in this phase is lower but the duration is significantly longer. The total impulse including the acoustic phase and the free-deflection phase is proportional to the impact velocity regardless of the structural stiffness. The rising time, however, is determined by structural stiffness and not sensitive to the initial impact velocity.

4. The non-dimensional diagrams for the permanent deflection of plate strips and stiffened panels as a function of the impact velocity, have been proved useful by comparison with ALE simulations. The simplicity of the diagrams makes them good candidates to be utilized in rules and standards concerned with design against extreme water slamming in ULS and ALS conditions.

REFERENCES

BAE, D.-M. & ZAKKI, A. F. 2011. Comparisons of Multi Material ALE and Single Material ALE in LS-DYNA for Estimation of Acceleration Response of Free-fall Lifeboat. *Journal of the Society of Naval Architects of Korea,* 48**,** 552-559.

BISHOP, R. E. & PRICE, W. G. 1979. *Hydroelasticity of ships*, Cambridge University Press.

DNVGL-OTG-13 2016. Prediction of air gap for column stabilised units. *offshore technical guidance.*

DNVGL-OTG-14 2016. Horizontal wave impact loads for column stabilised units. *Offshore Technical Guidance.*

FALTINSEN, O. M. 2000. Hydroelastic slamming. *Journal of Marine Science and Technology,* 5**,** 49-65.

FALTINSEN, O. M., KVÅLSVOLD, J. & AARSNES, J. V. 1997. Wave impact on a horizontal elastic plate. *Journal of Marine Science and Technology,* 2**,** 87-100.

HENKE, D. J. 1994. Transient response of plates to travelling loads with application to slamming damage. *International journal of impact engineering,* 15**,** 769-784.

JIANG, J. & OLSON, M. 1995. Rigid-plastic analysis of underwater blast loaded stiffened plates. *International journal of mechanical sciences,* 37**,** 843-859.

JONES, N. 2011. *Structural impact (second edition)*, Cambridge university press.

KVALSVOLD, J. & FALTINSEN, O. M. 1995. Hydroelastic modelling of wet deck slamming on multihull vessels.

QIN, Z. & BATRA, R. C. 2009. Local slamming impact of sandwich composite hulls. *International Journal of Solids and Structures,* 46**,** 2011-2035.

STENIUS, I., ROSÉN, A. & KUTTENKEULER, J. 2006. Explicit FE-modelling of fluid–structure interaction in hull–water impacts. *International Shipbuilding Progress,* 53**,** 103-121.

YU, Z. & AMDAHL, J. 2018. A review of structural responses and design of offshore tubular structures subjected to ship impacts. *Ocean Engineering,* 154**,** 177-203.

YU, Z., AMDAHL, J., GRECO, M. & XU, H. 2018a. Hydro-plastic response of beams and stiffened panels subjected to extreme water slamming, Part I: An analytical solution. *submitted to jounal*.

YU, Z., AMDAHL, J., GRECO, M. & XU, H. 2018b. Hydro-plastic response of beams and stiffened panels subjected to extreme water slamming, Part II: numerical verification and analysis. *Submitted to jounal*.

YU, Z., AMDAHL, J. & SHA, Y. 2018c. Large inelastic deformation resistance of stiffened panels subjected to lateral loading. *Marine Structures,* 59**,** 342-367.

ZHAO, R., FALTINSEN, O. & AARSNES, J. Water entry of arbitrary two-dimensional sections with and without flow separation. Proceedings of the 21st symposium on naval hydrodynamics, 1996. Trondheim, Norway, National Academy Press, Washington, DC, USA, 408-423.